

# Determining depletion interactions by contracting forces

Néstor M. de los Santos-López,<sup>1</sup> Gabriel Pérez-Ángel,<sup>1,\*</sup> Ramón Castañeda-Priego,<sup>2</sup> and José M. Méndez-Alcaraz<sup>3</sup>

<sup>1</sup>*Departamento de Física Aplicada, Cinvestav-Mérida, AP 73 “Cordemex”, 97310 Mérida, Yucatán, Mexico.*

<sup>2</sup>*División de Ciencias e Ingenierías, Campus León, Universidad de Guanajuato, Loma del Bosque 103, 37150 León, Guanajuato, Mexico.*

<sup>3</sup>*Departamento de Física, Cinvestav, Av. IPN 2508, Col. San Pedro Zacatenco, 07360 Gustavo A. Madero, Ciudad de México, Mexico.*

(Dated: October 8, 2021)

We introduce a general physical formulation that allows one to obtain uniquely the effective interactions by contracting the bare forces, even in highly concentrated systems. We tested it by studying depletion forces in two-dimensional binary and ternary colloidal mixtures with a total packing fraction up to 70%. Our result opens up the possibility of finding an efficient route to determine effective interactions at finite concentration and even at thermodynamic conditions near to meta-stable or out of equilibrium states.

Keywords: Depletion forces; entropic potentials, colloidal mixtures; hard-spheres.

The universal mechanism behind depletion forces in colloidal-like systems with large size-asymmetries and repulsive short-ranged interactions (predominantly in those systems whose main bare interaction is of the hard-core type) consists in the removal of small particles from the gap between two approaching large particles, leading to an imbalance of osmotic pressures on their internal and external faces, which drive them to stay together, giving rise to an increase in the entropy of the system that results in a strong, effective attraction at contact [1].

Analyzing the phenomenon of depletion forces beyond the dilute limit, it was found that a repulsive wall arises, just after the attractive well at contact [2, 3]. This effective repulsion is due to the formation of a layer of first neighbors of small particles around the large ones, when they are separated by a distance larger than the formers' diameter. This leads to an overpopulation of small particles in the gap between large ones, exactly the opposite of the depletion at smaller separations, driving again to an unbalance of osmotic pressures but now pushing the larger particles out. This barrier works as a kind of gate that controls the action of the attractive well at contact, and hence its enormous relevance for understanding, for example, the formation of colloidal clusters or the thermodynamic stability of the dispersion [4].

Theoretical, experimental, and simulation studies made it possible to understand in detail the behavior of depletion forces as a function of the concentration, size, and morphology of the involved species [1]. Depletion forces have been identified as the physical mechanism behind important thermodynamic processes and biological phenomena [1]. They have also led to the development of entropic engineering techniques as well [5, 6]. Currently, there has been a growing interest to understand the nature of depletion forces under non-equilibrium thermodynamic conditions [7] and thermodynamic meta-stable states [8–10].

There exist several theoretical approaches able to cap-

ture the complexity of depletion forces [1]. We refer below to the integral equations one [2, 3], which takes advantage of the covariance of the Ornstein-Zernike equation under contractions of the description. From the perspective of this theory, the structure of the particles of a single species in a mixture can be described with the effective potential resulting from the integration of the degrees of freedom of the remaining species, leading to the same distribution that would be obtained from a complete description of the system in terms of the bare potentials among all species.

When this theoretical approach is used in binary mixtures of large ( $l$ ) and small ( $s$ ) spheres, the resulting depletion potential between the former ones,  $\beta u_{ll}^{\text{eff}}(r)$ , after the contraction of the latter ones, can be written as [2, 3]

$$\beta u_{ll}^{\text{eff}}(r) = \beta u_{ll}(r) + [c_{ll}(r) - c_{ll}^{\text{eff}}(r)] + [b_{ll}^{\text{eff}}(r) - b_{ll}(r)], \quad (1)$$

or

$$\beta u_{ll}^{\text{eff}}(r) = \beta w_{ll}(r) + n_l \int_V c_{ll}^{\text{eff}}(r) h_{ll}(|\mathbf{r} - \mathbf{r}'|) d\mathbf{r}' + b_{ll}^{\text{eff}}(r), \quad (2)$$

with

$$\tilde{c}_{ll}^{\text{eff}}(q) = \tilde{c}_{ll}(q) + \frac{\tilde{c}_{ls}(q) n_s \tilde{c}_{sl}(q)}{1 - n_s \tilde{c}_{ss}(q)}. \quad (3)$$

Here,  $r$  is the distance between the centers of the spheres,  $q$  the wave-number and  $\tilde{f}(q)$  the Fourier-transform of  $f(r)$ .  $n_i$  and  $\beta = 1/k_B T$  are the number density of species  $i$  and the inverse of the thermal energy, respectively, with  $k_B$  being the Boltzmann constant and  $T$  the absolute temperature. The bare interaction potential between particles of species  $i$  and  $j$  in the mixture ( $i, j = s, l$ ) is  $u_{ij}(r)$ , whereas  $h_{ij}(r)$ ,  $c_{ij}(r)$ , and  $b_{ij}(r)$  are the total, direct and bridge correlations, respectively

[11]. The superscript *eff* denotes the corresponding effective functions (after the contraction of the description). The spatial distribution of large particles must be the same at both levels of description, i.e.,  $h_{ll}^{\text{eff}}(r) = h_{ll}(r)$ . The potential of mean force between large particles is  $\beta w_{ll}(r) = -\ln g_{ll}(r)$ , with  $g_{ll}(r) = h_{ll}(r) + 1$  being the corresponding radial distribution function [11].

Equation (1), together with Eq. (3), highlights the fact that the effective potential among large spheres emerges from the particle correlations, i.e., the depletion potential is then given by the bare one plus terms depending on the correlations between large particles mediated by the small ones. An interesting and natural result obtained from Eq. (2), and confirmed by independent experiments and molecular simulations [12], is that the effective potential tends to the potential of mean force when only a few large particles are present (the leading term in  $b_{ll}^{\text{eff}}(r)$  is quadratic in  $n_l$  [11]), even for high concentrations of small particles. The correlation terms in Eq. (1) have been evaluated under many approximations, and their predictions systematically tested for self-consistency by ensuring the equality of the radial distribution functions obtained by both routes, simulating the complete mixture with the bare potentials and the effective monodisperse system of large particles with the depletion interaction [8, 12]. As far as we know, there are no experimental or simulation schemes that allow us to get the effective potential among large spheres at finite concentration [8].

As pointed out above, the direct comparison between theoretical effective interactions and molecular simulations has only been possible in the diluted case, i.e., when  $n_l \rightarrow 0$  and  $u_{ll}^{\text{eff}}(r) \rightarrow w_{ll}(r)$ , in which depletion forces can be obtained from the simulations, for example, by fixing two large particles at a given separation and adding the projections on the line connecting their centers of the transfer of momentum per unit time due to the collisions between them and the small particles [3, 13]. This is, in fact, the standard protocol to extract an effective potential from molecular simulations even in those cases where the small particles undergo a phase transition or are near a percolated-like state [10]. A comparison has not been possible for concentrated systems due to the lack of a physical approach, which can obtain effective interactions from, for example, molecular dynamics simulations. Thus, this letter aims to introduce a general physical formulation that allows us to obtain the depletion forces even when the concentration of the non-depleted species is not negligible.

In the following, we will show that the effective interactions, particularly the depletion one, can be uniquely determined from the forces' contraction. Let us assume a colloidal mixture composed of  $N_l$  large spheres and  $N_s$  small ones, generically denoted with the subindex  $s$  for the moment, but leaving open the possibility of several small species. The total force exerted on the  $i$ -th large

particle at time  $t$  is

$$\mathbf{F}_i^l(\mathbf{r}_i) = \sum_{j \neq i}^{N_l} \mathbf{f}_{ji}^{ll}(\mathbf{r}_{ji}) + \sum_{k=1}^{N_s} \mathbf{f}_{ki}^{sl}(\mathbf{r}_{ki}), \quad (4)$$

where  $\mathbf{f}_{ji}^{ll}(\mathbf{r}_{ji})$  is the bare force exerted by the  $j$ -th large particle and  $\mathbf{f}_{ki}^{sl}(\mathbf{r}_{ki})$  the one exerted by the  $k$ -th small particle. Now, in the contracted description, we rewrite equation (4) in the form,

$$\langle \mathbf{F}_i^l(\mathbf{r}_i) \rangle_s = \sum_{j \neq i}^{N_l} \mathbf{G}_{ji}^{ll}(\mathbf{r}_{ji}), \quad (5)$$

where  $\langle \mathbf{F}_i^l(\mathbf{r}_i) \rangle_s$  is the average of  $\mathbf{F}_i^l(\mathbf{r}_i)$  over the configurations of the small particles in the fixed field of the large ones. Therefore,  $\mathbf{G}_{ji}^{ll}(\mathbf{r}_{ji}) = G_{ji}^{ll}(\mathbf{r}_{ji}) \hat{\mathbf{r}}_{ji}$  must correspond to the effective force obtained from Eqs. (1) or (2), i.e.,  $\mathbf{G}_{ji}^{ll}(\mathbf{r}_{ji}) = -\nabla u_{ll}^{\text{eff}}(r_{ji})$ . Here, the time dependence enters into equations through the particle positions;  $\mathbf{r}_i$  is the position of particle  $i$  concerning the frame of reference of the laboratory and  $\mathbf{r}_{ji} = \mathbf{r}_i - \mathbf{r}_j$  the position of particle  $i$  respect to particle  $j$ , being  $r_{ji}$  the distance between their centers at time  $t$ . Also  $\hat{\mathbf{r}}_{ji}$  is a unitary vector along  $\mathbf{r}_{ji}$ , and  $\nabla = d/dr_{ji} = \hat{\mathbf{r}}_{ji} d/dr_{ji}$ .

Small particles were integrated out from the description by going from Eqs. (4) to (5), as they go from being explicit components of the system to a part of the supporting environment, after averaging over their configurations. Their effects are implicitly included in the effective force  $\mathbf{G}_{ji}^{ll}(\mathbf{r}_{ji})$  between large particles. The idea is to evaluate  $\mathbf{F}_i^l(\mathbf{r}_i)$  using Eq. (4) and then take it into Eq. (5) to get  $\mathbf{G}_{ji}^{ll}(\mathbf{r}_{ji})$ . The instantaneous values of  $\mathbf{F}_i^l(\mathbf{r}_i)$  obtained from Eq. (4) are noisy, even if they are obtained through a deterministic simulation run, and satisfy Eq. (5) only over long times. Instead, they may be described by the stochastic equation,

$$\mathbf{F}_i^l(\mathbf{r}_i) = \sum_{j \neq i}^{N_l} \mathbf{G}_{ji}^{ll}(\mathbf{r}_{ji}) + \mathbf{D}_i^l(t), \quad (6)$$

where  $\mathbf{D}_i^l(t)$  corresponds to the non-systematic part of the instant forces, due to the constant tapping of small particles on the large ones, expected to be a noisy term with zero mean,  $\langle \mathbf{D}_i^l(t) \rangle_s = 0$ , and finite variance (irrelevant for the determination of the effective interaction). The force  $\mathbf{F}_i^l(\mathbf{r}_i)$  in Eq. (6) can be interpreted as the noisy result of a measurement and the  $\mathbf{G}_{ji}^{ll}(\mathbf{r}_{ji})$ 's as fitting functions for it, being  $\mathbf{D}_i^l(t)$  the instant deviations between measured and fitted values. Therefore, the values of  $\mathbf{G}_{ji}^{ll}(\mathbf{r}_{ji})$  can be obtained using the least-squares method [14].

To illustrate the applicability of the contraction of the forces given by Eq. (6), we now study the depletion forces in a two-dimensional colloidal system. After getting  $\mathbf{F}_i^l(\mathbf{r}_i)$  from Eq. (4), we split Eq. (6) into its  $x$ - and

$y$ -components,

$$\begin{aligned} F_{i,x}^l(\mathbf{r}_i) &= \sum_{j \neq i}^{N_l} G_{ji}^{ll}(r_{ji}) \cos \theta_{ji} + D_{i,x}^l(t) \\ F_{i,y}^l(\mathbf{r}_i) &= \sum_{j \neq i}^{N_l} G_{ji}^{ll}(r_{ji}) \sin \theta_{ji} + D_{i,y}^l(t), \end{aligned} \quad (7)$$

with  $\theta_{ji}$  being the angle between  $\mathbf{r}_{ji}$  and the  $x$ -direction. To proceed numerically we discretize the distance  $r_{ji}$  into  $C$  classes,

$$r_{ji} \rightarrow r_n = n\delta, \quad \text{if } r_n \leq r_{ji} < r_{n+1}, \quad (8)$$

where  $\delta$  is the class-size and  $n = 0, \dots, C-1$ , assuming  $r_{max} = C\delta$  as the range of the depletion effects. Therefore, the forces become

$$\begin{aligned} F_{i,x}^l(\mathbf{r}_i) &= \sum_{n=0}^{C-1} A_n^i G_{ji}^{ll}(r_n) + D_{i,x}^l(t) \\ F_{i,y}^l(\mathbf{r}_i) &= \sum_{n=0}^{C-1} B_n^i G_{ji}^{ll}(r_n) + D_{i,y}^l(t), \end{aligned} \quad (9)$$

with

$$A_n^i = \sum_{j \neq i}^{N_{l,n}} \cos \theta_{ji} \quad \text{and} \quad B_n^i = \sum_{j \neq i}^{N_{l,n}} \sin \theta_{ji}. \quad (10)$$

The sub-index  $n$  in the upper limits of the sums indicates that these are carried out only over those  $j$ -values with  $r_{ij}$  being in class  $n$ . In matrix notation, one gets

$$\mathbb{F}_x = \mathbb{A}\mathbb{G} + \mathbb{D}_x \quad \text{and} \quad \mathbb{F}_y = \mathbb{B}\mathbb{G} + \mathbb{D}_y. \quad (11)$$

The matrices  $\mathbb{F}_x$ ,  $\mathbb{F}_y$ ,  $\mathbb{D}_x$ , and  $\mathbb{D}_y$  have only one column with  $\mathcal{N}N_l$  rows, being  $\mathcal{N}$  the number of simulated configurations used to gather statistics, with typical values of  $10^6$  or more, since one accumulates in the matrix arrangements the values obtained for each of the analyzed configurations, for each large particle. The matrix  $\mathbb{G}$  has one column with  $C$  rows, typically about  $10^2$ . The matrices  $\mathbb{A}$  and  $\mathbb{B}$  are arrays with the same number of rows as  $\mathbb{F}_x$  and  $\mathbb{F}_y$ , and  $C$  columns.

The linear equations represented by (11) are highly over-determined, since the rows are much more than the columns. To overcome this difficulty, we use the least-squares method (LS) [14], demanding the values of  $\mathbb{G}$ 's elements to minimize the ones of  $\mathbb{D}_x^T \mathbb{D}_x$  and  $\mathbb{D}_y^T \mathbb{D}_y$  simultaneously. This leads to equations,

$$\mathbb{A}^T \mathbb{A} \mathbb{G} = \mathbb{A}^T \mathbb{F}_x \quad \text{and} \quad \mathbb{B}^T \mathbb{B} \mathbb{G} = \mathbb{B}^T \mathbb{F}_y, \quad (12)$$

which represent closed and well-defined systems of  $C$  linear equations with  $C$  variables, which are solved using Singular Value Decomposition (SVD), since the matrices  $\mathbb{A}^T \mathbb{A}$  and  $\mathbb{B}^T \mathbb{B}$  may be singular or close to it [14]. We

carry out the same procedure for both  $\mathbb{F}_x$  and  $\mathbb{F}_y$  independently, and so one gets two different solutions for  $\mathbb{G}$ . Clearly, a comparison between them gives some validation to our approach; in all cases, we found them equal up to statistical fluctuations. The values shown below are the average of both solutions. At this point, we should set the details of the system under consideration.

We simulate ternary mixtures composed of one species of large disks, and two species of small ones, here denoted as  $s1$  and  $s2$ , with diameters  $\sigma_l$ ,  $\sigma_{s1} = \sigma_l/3$ , and  $\sigma_{s2} = \sigma_l/5$ , respectively. The bare interaction potential between disks is given by the Weeks-Chandler-Andersen (WCA) soft-potential [15],

$$\begin{aligned} u_{ij}(r_{ij}) &= 4\epsilon \left[ \left( \frac{\sigma_{ij}}{r_{ij}} \right)^{12} - \left( \frac{\sigma_{ij}}{r_{ij}} \right)^6 \right] + \epsilon \quad \text{if } r_{ij} < 2^{1/6} \sigma_{ij} \\ &= 0 \quad \text{otherwise,} \end{aligned} \quad (13)$$

where  $\sigma_{ij} = (\sigma_i + \sigma_j)/2$ , which provides a reasonable approach to hard particles [16]. We perform Molecular Dynamics simulations in a box of length  $L$  and area  $A$  with periodic boundary conditions in the bi-dimensional canonical ensemble at a reduced temperature  $T^* \equiv k_B T / \epsilon = 1.0$ . Length, mass, and time scales are given by  $\sigma_l$ ,  $m_l$ , and  $\sqrt{m_l \sigma_l^2 / k_B T}$ , respectively. The mass of a large disk is  $m_l$ , while the masses of the small ones keep the same proportion as their areas. The total number of particles is  $N = N_l + N_{s1} + N_{s2}$ , and  $\phi_i = N_i \pi \sigma_i^2 / 4A$  is the surface fraction of the  $i$ -th species, with  $\phi = \phi_l + \phi_{s1} + \phi_{s2}$  being the total packing fraction.

The simulation begins by randomly placing the disks without overlapping and it is carried out using the velocity-Verlet algorithm [17]. To keep the temperature constant, a simple velocity rescaling criterion is used. The transient part is run until equilibrium is reached, checked by monitoring the excess energy, and waiting until it becomes stationary; to avoid possible aging effects, it is ensured that the mean-square displacements and radial distribution functions (RDFs) do not depend on the transient time in systems with  $\phi$  above 60%. We have also verified that the initial and final RDFs for the production runs are alike. Afterwards, the calculation of the forces starts. Applying the test of self-consistency, we also simulate, using molecular dynamics, the effective monodisperse systems of large disks interacting via the numerically extracted depletion forces. The RDFs for those monodisperse runs are then compared with their counterparts in the original simulations for the ternary mixture with the bare WCA interaction.

Figure 1 shows the depletion force, times  $\beta \sigma_l$ , as a function of the distance between the centers of large particles for three systems with  $\phi = 0.6$  and  $\phi_l = 0.2$  fixed. Insets show closer details around the depletion well and barrier. The extreme repulsion about contact corresponds to the bare potential (the first term on the right side of Eq. (1)). The following attractive well corresponds to the depletion

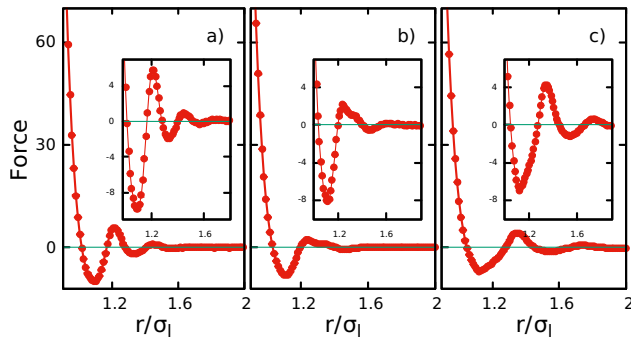


FIG. 1. Depletion force, times  $\beta\sigma_l$ , for three systems with  $\phi = 0.6$ , having  $\phi_l = 0.2$  and: (a)  $\phi_{s1} = 0$  and  $\phi_{s2} = 0.4$ ; (b)  $\phi_{s1} = \phi_{s2} = 0.2$ ; (c)  $\phi_{s1} = 0.4$  and  $\phi_{s2} = 0.0$ . Insets show closer details around the depletion well and barrier.

attraction that can be understood quite well in terms of the Asakura-Oosawa limit of Eqs. (1) and (3) [2, 3]. In the bidisperse case, its depth is proportional to the concentration of depletants and the size ratio  $\sigma_l/\sigma_s$ , while its range is the size of depletants. It is followed by the repulsive barrier arising from the accumulation of depletants in the first neighbors layer around large particles, a complex and poorly studied effect contained in the last two terms on the right side of Eq. (1) [3]; it is, however, of importance to understand the cluster formation in competing interaction fluids [18]. At first glance, its amplitude and range seem to behave like those of the attractive well, in the bidisperse case. Nevertheless, the main consequence of adding a second species of depletants is to reduce and flatten this barrier in such a way that polydispersity seems to be a control parameter of this gate [19]. A similar outcome has been observed in binary mixtures of large spheres and small spherocylinders, of diameter  $\sigma$  and length  $L$ , which roughly behave like two spherical depletant species of diameters  $\sigma$  and  $L$  [20].

Figure 2 shows the RDFs between large particles for the three systems reported in Fig. 1. We include a comparison for the original mixture with the WCA bare interaction and simulations results for the effective monodisperse system of large particles interacting with the depletion forces shown in Fig. 1. Insets show closer details around the second minimum of  $g(r)$ , where we found the largest deviations. The excellent agreement between RDFs confirms that the contraction process, which is carried out by going from Eqs. (4) to (5), captures all the depletion effects correctly.

The description is contracted within the integral equations formalism by demanding  $g_{ll}(r)$  to be invariant. In contrast, the approach presented here requires  $\mathbf{F}_i^l(\mathbf{r}_i)$  not to change by going from Eqs. (4) to (6). Both conditions are actually equivalent, as suggested by the excellent agreement shown in Fig. 2. The potential of mean force is defined to reproduce the mean force acting on a

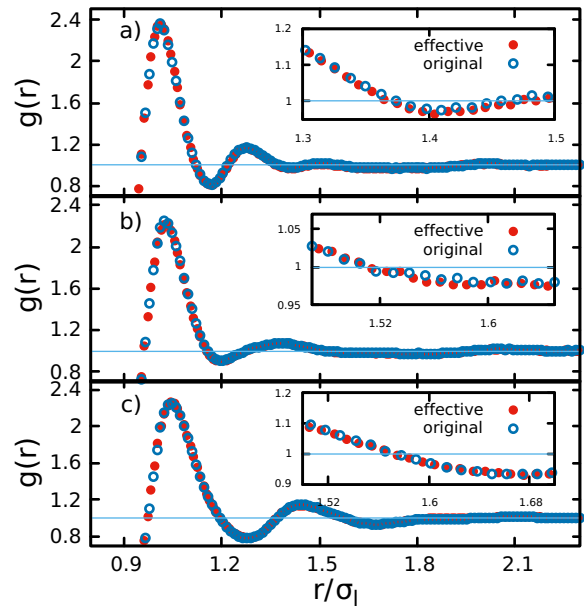


FIG. 2. Radial distribution functions between large disks for the three systems in Fig. 1. Insets show closer details around the second minimum. The blue circles are the simulations results for the original mixture with the WCA bare interaction and the red circles the simulations results for the effective monodisperse system of large particles interacting with the depletion forces shown in Fig. 1.

large particle, i.e.,  $\langle \mathbf{F}_i^l(\mathbf{r}) \rangle = -\nabla w_{ll}(r)$  [21]. Therefore, by demanding the invariance of  $\mathbf{F}_i^l(\mathbf{r}_i)$  under contractions of the description, we also impose that of  $g_{ll}(r)$ . However,  $w_{ll}(r)$  should not be confused with  $u_{ll}^{\text{eff}}(r)$ , as it becomes clear from Eq. (2) and Fig. 3, since the ensemble average  $\langle \mathbf{F}_i^l(\mathbf{r}) \rangle$  is over the configurations of large and small particles.

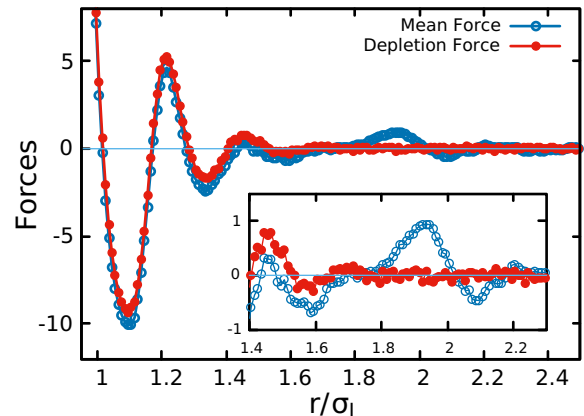


FIG. 3. Depletion force (red circles) and mean force (blue circles), times  $\beta\sigma_l$ , between large particles for a system with  $\phi = 0.7$ , having  $\phi_l = 0.4$ ,  $\phi_{s1} = 0$ , and  $\phi_{s2} = 0.3$ . The lines are just a guide for the eye.

Figure 3 shows the depletion and mean forces, times  $\beta\sigma_l$ , between large particles for a system with  $\phi = 0.7$ ,

having  $\phi_l = 0.4$ ,  $\phi_{s1} = 0$ , and  $\phi_{s2} = 0.3$ . The mean force was obtained by deriving  $\beta w_{ll}(r) = -\ln g_{ll}(r)$  numerically using the 3-7 Savitsky-Golay filter [14]. The discrepancies between the two interactions are evident in this concentrated system, mainly around the layer of second neighbors of large particles,  $r/\sigma_l \approx 2$ , where the mean force shows a structure not included in the depletion one. This is produced by the bare interaction between large disks, not contained in the correlations mediated by small ones, which fade at shorter distances. On the other hand, Fig. 3 also reveals that the potential of mean force still approximates the depletion interactions at small distances quite well, albeit with a small systematic deviation, even at those concentrations.

As in the case of the integral equations theory of depletion forces, the physical approach reported here is much more general than the example used to illustrate it. In principle, both approaches may obtain any effective interaction resulting from reducing the description of the system, be it species, the number of particles, geometry or dimensionality. However, its implementation must be adapted to each situation. In particular, we have shown its outstanding performance in concentrated binary and ternary mixtures of hard-like particles, where entropic depletion is the dominant mechanism behind the interaction between larger particles. However, its use to study more interesting and sophisticated situations, for example, effective interactions near thermodynamic instabilities, is in progress. Last, but not least, we should mention that this approach can also be used in, for example, confocal videomicroscopy experiments to determine the effective forces between colloids.

Authors thank Conacyt for financial support (Grant No. 237425). GP-A thanks Conacyt for financial support (Grant A1-S-46572).

---

\* gperez@cinvestav.mx

[1] H. N. W. Lekkerkerker and R. Tuinier, *Colloids and the Depletion Interaction* (Springer, 2011).

- [2] J. M. Méndez-Alcaraz and R. Klein, *Phys. Rev. E* **61**, 4095 (2000).
- [3] R. Castañeda-Priego, A. Rodríguez-López, and J. M. Méndez-Alcaraz, *Phys. Rev. E* **73**, 051404 (2006).
- [4] N. E. Valadez-Pérez, Y. Liu, and R. Castañeda Priego, *Phys. Rev. Lett.* **120**, 248004 (2018).
- [5] A. D. Dinsmore, J. C. Crocker, and A. G. Yodh, *Curr. Opin. Colloid Interface Sci.* **3**, 5 (1998).
- [6] K.-H. Lin, J. C. Crocker, V. Prasad, A. Schofield, D. A. Weitz, T. C. Lubensky, and A. G. Yodh, *Phys. Rev. Lett.* **85**, 1770 (2000).
- [7] J. Dzubiella, H. Löwen, and C. N. Likos, *Phys. Rev. Lett.* **91**, 248301 (2003).
- [8] E. López-Sánchez, C. D. Estrada-Álvarez, G. Pérez-Ángel, J. M. Méndez-Alcaraz, P. González-Mozuelos, and R. Castañeda-Priego, *J. Chem. Phys.* **139**, 104908 (2013).
- [9] P. J. Lu, E. Zaccarelli, F. Ciulla, A. B. Schofield, F. Sciortino, and D. A. Weitz, *Nature* **453**, 499 (2008).
- [10] N. Gnan, E. Zaccarelli, and F. Sciortino, *Nature Communications* **5**, 3267 (2014).
- [11] J.-P. Hansen and I. R. McDonald, *Theory of Simple Liquids*, 2nd ed. (Academic Press, 1986).
- [12] J. Perera-Burgos, J. M. Méndez-Alcaraz, G. Pérez-Ángel, and R. Castañeda-Priego, *J. Chem. Phys.* **145**, 104905 (2016).
- [13] T. Biben, P. Bladon, and D. Frenkel, *J. Phys.: Condens. Matter* **8**, 10799 (1996).
- [14] W. H. Press, B. P. Flannery, S. A. Teukolsky, and W. T. Vetterling, *Numerical Recipes in C: The Art of Scientific Computing*, 2nd ed. (Cambridge University Press, 1992).
- [15] J. D. Weeks, D. Chandler, and H. C. Andersen, *J. Chem. Phys.* **54**, 5237 (1971).
- [16] M. Schmiedeberg, T. K. Haxton, S. R. Nagel, and A. J. Liu, *Europhys. Lett.* **96**, 36010 (2011).
- [17] M. P. Allen and D. J. Tildesley, *Computer Simulation of Liquids* (Oxford, 1987).
- [18] P. D. Godfrin, N. E. Valadez-Pérez, R. Castañeda-Priego, N. J. Wagner, and Y. Liu, *Soft Matter* **10**, 5061 (2014).
- [19] R. Roth and M. Kinoshita, *The Journal of Chemical Physics* **125**, 084910 (2006).
- [20] P. González-Mozuelos, J. M. Méndez-Alcaraz, and R. Castañeda-Priego, *J. Chem. Phys.* **123**, 214907 (2005).
- [21] G. D. J. Phillies, *Elementary Lectures in Statistical Mechanics* (Springer, 2000).